GA–A27787

DEVELOPING PHYSICS BASIS FOR THE RADIATIVE SNOWFLAKE DIVERTOR IN DIII-D

By
V.A. SOUKHANOVSKII, S.L. ALLEN, M.E. FENSTERMACHER, D.N. HILL, C.J. LASNIER, M.A. MAKOWSKI, A.G. McLEAN, W.H. MEYER, D.D. RYUTOV, E. KOLEMEN, R.J. GROEBNER, A.W. HYATT, A.W. LEONARD, T.H, OSBORNE, T.W. PETRIE, J.A. BOEDO, and J.G. WATKINS

APRIL 2014

GENERAL ATOMICS

DISCLAIMER

GA–A27787

DEVELOPING PHYSICS BASIS FOR THE RADIATIVE SNOWFLAKE DIVERTOR IN DIII-D

By
V.A. SOUKHANOVSKII,* S.L. ALLEN,* M.E. FENSTERMACHER,* D.N. HILL,* C.J. LASNIER,* M.A. MAKOWSKI,* A.G. McLEAN,* W.H. MEYER,* D.D. RYUTOV,* E. KOLEMEN,† R.J. GROEBNER, A.W. HYATT, A.W. LEONARD, T.H, OSBORNE, T.W. PETRIE, J.A. BOEDO,‡ and J.G. WATKINS#

This is a preprint of the synopsis for a paper to be presented at the Twenty-Fifth IAEA Fusion Energy Conf., October 13-18, 2014 in Saint Petersburg, Russia.

*Lawrence Livermore National Laboratory, Livermore, California.
†Princeton Plasma Physics Laboratory, Princeton, New Jersey.
‡University of California San Diego, La Jolla, California.
#Sandia National Laboratories, Livermore, California.

Work supported by
the U.S. Department of Energy
under DE-AC52-07NA27344, DE-AC02-09CH11466,
DE-FC02-04ER54698, and DE-FG02-07ER54917

GENERAL ATOMICS PROJECT 30200
APRIL 2014

GENERAL ATOMICS

Developing Physics Basis for the Radiative Snowflake Divertor in DIII-D

EX-D

V.A. Soukhanovskii[1], S.L. Allen[1], M.E. Fenstermacher[1], D.N. Hill[1], C.J. Lasnier[1], M.A. Makowski[1], A.G. McLean[1], W.H. Meyer[1], D.D. Ryutov[1], E. Kolemen[2], R.J. Groebner[3], A.W. Hyatt[3], A.W. Leonard[3], T.H. Osborne[3], T.W. Petrie[3], J.A. Boedo[4], and J.G. Watkins[5]
E-mail: vlad@llnl.gov

[1]Lawrence Livermore National Laboratory, 7000 East Ave, Livermore, CA 94550, USA
[2]Princeton Plasma Physics Laboratory, PO Box 451, Princeton, NJ 08543-0451, USA
[3]General Atomics, PO Box 85608, San Diego, CA 92186-5608, USA
[4]University of California San Diego, 9500 Gilman Dr., La Jolla, CA 92093-0417, USA
[5]Sandia National Laboratories, PO Box 969 Livermore, California 94551-0969, USA

Recent DIII-D studies show the snowflake (SF) divertor [1] enables significant manipulation of divertor heat transport for power spreading in attached and radiative divertor conditions, between and during edge localized modes (ELMs), while maintaining good H-mode confinement (H_{98y2}>1). Results include: 1) Enhanced heat transport through the low poloidal field null-point region and divertor legs resulting in increased scrape-off layer (SOL) width (Fig. 1); 2) Direct measurements of divertor null-region poloidal beta β_p>>1, supporting the theoretically proposed instability mechanism leading to fast convective heat redistribution between strike points, which is especially efficient during ELMs; 3) In radiative SF divertor regimes, a significant reduction of peak heat fluxes between and during ELMs.

Enhanced transport through the null point region and heat spreading over additional strike points (SPs) between ELMs is inferred from the heat flux profile and SOL width analysis of attached SF divertor conditions in H-mode discharges (I_p=1.2 MA, P_{NBI}=3-5 MW, and Bx∇B down). The Eich function [2] fits to parallel heat flux profiles $q_{||}(r)$ are used to assess heat diffusion due to the increased connection length in the SF configuration, and changes in radial heat transport affecting the outer common SOL width. In nearly-exact SF configurations, with a small distance d_{XX} between nulls (e.g., $d_{XX}/a \leq 0.15$, where a is the minor radius), the integral SOL width is increased: λ_{SOL}~3.0-3.2 mm (cf. λ_{SOL}~2.5 mm in the standard divertor [3]). Increased are both the Gaussian heat diffusion component into the private flux region, apparently due to the connection length that is increased by a factor 2–4 in the SF, and the SOL common flux region component, indicating increased radial transport. In SF configuration variants, the SF-minus and SF-plus, with $d_{XX}/a \geq 0.15$, the SOL width is not necessarily increased, and geometry effects dominate divertor heat deposition. The deposited heat flux is reduced due to the increased plasma-wetted area (poloidal magnetic flux expansion). The parallel heat transport is mostly affected by heat spreading over additional SPs, and increased

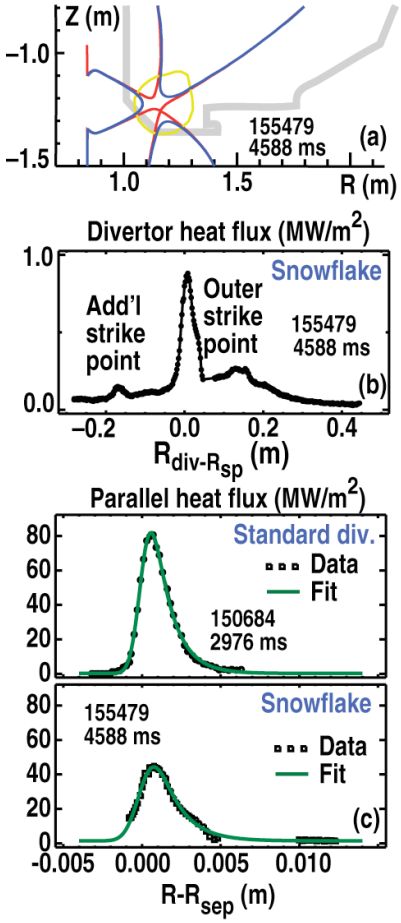

Fig. 1. (a) Near-exact SF configuration, with a contour around the X-point region showing the extent of low $|B_p/B_{pm}|$ = 0.10 region, where the poloidal magnetic field B_p is normalized to its midplane B_{pm} value, (b) divertor heat flux profile, (c) Parallel heat flux $q_{||}$ profile projected to midplane, and the Eich function fit, for the standard and SF configurations.

connection length. The amount of heat flux measured at additional strike points is often proportional to input power and divertor density.

Recent measurements are consistent with the theoretically predicted SF property critical for ELM heat transport, i.e. the fast convective plasma redistribution through the null point region due to the onset of a flute-like instability. The poloidal beta in the null-region $\beta_p = P_k/P_m >> 1$ (where P_m is the poloidal magnetic pressure and P_k is the plasma kinetic pressure), and the magnitude and extent of the high β_p region were directly inferred from the divertor Thomson scattering measurements of electron pressure profiles and poloidal field distribution. The measured divertor $\beta_p \sim 50–100$ was about 2–3 orders of magnitude higher than the midplane β_p, and the high β_p region was broader in the SF configuration. During an ELM, the β_p is increased up to an order of magnitude, in agreement with the theoretical estimates of the instability β_p threshold based on the ideal MHD theory [4].

Type I ELM heat transport is also significantly affected by the SF divertor geometry. The extended low poloidal magnetic field region affects pedestal magnetic properties, e.g., the magnetic shear and q_{95} increase by up to 30%, and weakly affects the kinetic profiles, e.g., the pedestal energy remains constant. These changes, however, are not sufficient to affect the pealing-ballooning mode stability in the H-mode discharges, as the ELM frequency and size are changed by 10%–20%. A significant reduction in stored energy lost per ELM, from W_{ELM}/W_{PED}~ 12% to ~6%, due to the reduction in the conduction loss channel [5] with increased pedestal collisionality is observed. The ELMs deposited energy preferentially in the inner divertor in both the standard and the SF configurations. In the attached divertor, the peak ELM heat flux was reduced from 4–8 MW/m^2 in the standard *inner* divertor to 1–3 MW/m^2 in the SF-minus configuration. In the SF-plus configuration, outer peak heat flux in both the standard and SF configurations was dominated by a similar heat flux deposition pattern in the far SOL with minimal impact on the near-SOL.

In the radiative SF divertor with D_2 seeding, a significant peak heat flux reduction between and during ELMs was demonstrated. In the SF-minus divertor, similarly to NSTX [6], the heat flux in the primary outer SP became negligible between and during ELMs, while in the secondary SP, peak heat flux was lowered by 30%–60% between and during ELMs (cf. the standard partially detached SP). Carbon divertor radiation was more broadly distributed in the SF-minus. In the radiative SF-plus with D_2 or neon seeding, peak divertor loads in the inner and outer SPs were significantly reduced (to below 0.5 MW/m^2). Radiated power was distributed over all divertor SPs, and with increased collisionality (density), the radiation fronts moved up towards the null region (Fig. 2).

In summary, recent results from DIII-D, namely, enhancement of heat transport and heat redistribution among additional strike points, and divertor heat flux reduction between and during ELMs in the SF with gas seeding, support the radiative SF divertor as a promising concept for tokamak power exhaust.

This work was performed under the auspices of the US Department of Energy under DE-AC52-07NA27344, DE-AC02-09CH11466, DE-FC02-04ER54698, DE-FG02-07ER54917, and DE-AC04-94AL85000.

[1] D.D. Ryutov, Phys. Plasmas **14** (2007) 064502; Plasma Phys. Controlled Fusion **54** (2012) 124050
[2] T. Eich, et al., Phys. Rev. Lett. **107** (2011) 215001
[3] M. A. Makowski et al., Phys. Plasmas **19**, 056122 (2012)
[4] W.A. Farmer and D.D. Ryutov, Phys. Plasmas **20** (2013) 092117
[5] D.N. Hill et al., Nucl. Fusion **53** (2013) 104001
[6] V.A. Soukhanovskii et al., Phys. Plasmas **16** (2009) 022501

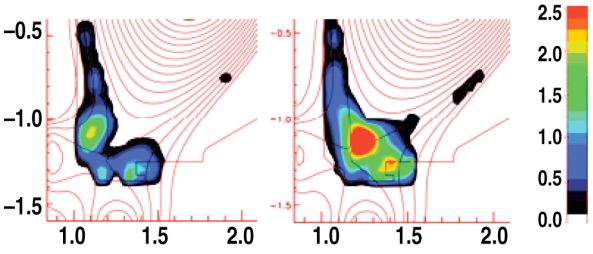

Fig. 2. Divertor radiated power distribution in the attached SF-plus (n_e=5x10^{19} m^{-3}) and radiative SF-plus (n_e=7.3x10^{19} m^{-3}).